Genetic analysis of age-dependent defects of the *Caenorhabditis elegans* touch receptor neurons

Chun-Liang Pan[a,b,1], Chiu-Ying Peng[b], Chun-Hao Chen[b], and Steven McIntire[a,1]

[a]Ernest Gallo Clinic and Research Center and Department of Neurology, University of California, San Francisco, Emeryville, CA 94608; [b]Institute of Molecular Medicine, College of Medicine, National Taiwan University, Taipei 10002, Taiwan

Edited by Mu-ming Poo, University of California, Berkeley, California, and approved April 19, 2011 (received for review August 8, 2010)

Although many genes have been implicated in the pathogenesis of common neurodegenerative diseases, the genetic and cellular mechanisms that maintain neuronal integrity during normal aging remain elusive. Here we show that *Caenorhabditis elegans* touch receptor and cholinergic neurons display age-dependent morphological defects, including cytoskeletal disorganization, axon beading, and defasciculation. Progression of neuronal aging is regulated by DAF-2 and DAF-16 signaling, which also modulate adult life span. Mutations that disrupt touch-evoked sensory activity or reduce membrane excitability trigger accelerated neuronal aging, indicating that electrical activity is critical for adult neuronal integrity. Disrupting touch neuron attachment to the epithelial cells induces distinct neurodegenerative phenotypes. These results provide a detailed description of the age-dependent morphological defects that occur in identified neurons of *C. elegans*, demonstrate that the age of onset of these defects is regulated by specific genes, and offer experimental evidence for the importance of normal levels of neural activity in delaying neuronal aging.

extracellular matrix | insulin signaling | ion channels | mechanosensory neurons | neurodegeneration

In humans, aging is accompanied by the progressive decline in behavioral and cognitive functions. Studies have shown that the numbers of neurons in most cortical regions of the human brain are relatively preserved during aging (reviewed in ref. 1). Although reduced synaptic numbers or white matter density has been proposed as the cellular basis for age-related behavioral decline (reviewed in ref. 1), descriptions of neuronal morphology during aging remain inconsistent, and a detailed record of normal neuronal aging is largely lacking.

In the nematode *Caenorhabditis elegans*, age-dependent morphological changes are widespread in somatic tissues (2–4). However, there is little evidence for neuronal aging in *C. elegans* (3). The observations by Herndon et al. (3) suggest that neuronal loss or axon guidance defects do not occur in the aging *C. elegans* nervous system. It was also shown that whereas nuclear membranes of other somatic cell nuclei undergo drastic age-dependent deterioration, those of neuronal nuclei remain relatively intact in aging animals (4).

There is, however, a clear age-dependent behavioral decline in *C. elegans*, including decrease in pharyngeal pumping, locomotion and chemotaxis (5). Evidence suggests that failure in neuronal activity could play a direct role in age-dependent behavioral deterioration. Cai and Sesti (6) showed that age-dependent oxidation of the *C. elegans* potassium channel KVS-1 causes sensory loss and that protection of neuronal KVS-1 from oxidation rescues age-dependent decline in chemotaxis behavior. Electrical activity has been shown to be important for neuronal development (7) and was recently implicated in the survival or maintenance of adult mammalian and *Drosophila* neurons (8, 9). However, it is unclear how electrical activity promotes the integrity of adult neurons.

In this paper, we address whether more subtle, subcellular changes occur in the aging *C. elegans* nervous system. Our results indicate that *C. elegans* neurons do develop age-dependent changes. Moreover, we show that electrical activity and normal attachment to the neighboring epithelial cells are required for the maintenance of adult touch receptor neurons.

Results

Age-Dependent Neuronal Defects in *C. elegans*. To further characterize age-dependent changes in *C. elegans* neurons, we focused on the ALM and PLM touch receptor neurons, two classes of bilaterally symmetric mechanosensory neurons that respond to light touch. These neurons extend a long anterior process that makes synaptic contact with other neurons and a short posterior process with no known function (Fig. 1*A*). The ALM process extends a synaptic branch into the nerve ring, the major *C. elegans* neuropil, and the PLM process extends a collateral branch to make synaptic contact in the ventral nerve cord (10). Whereas the ALM soma was typically round or oval in young adult animals, it became progressively irregularly shaped in old animals and often elaborated aberrant protrusions (Fig. 1 *B* and *C*). Immunostaining for acetylated α-tubulins revealed that these aberrant protrusions contain acetylated microtubules (Fig. 1*B*). In young animals, microtubule bundles were oriented in parallel, whereas in old animals with irregular ALM somas, microtubule bundles appeared more disorganized (Fig. 1*B*). We also observed age-dependent defects in the ALM and PLM processes (Fig. 1 *E–K* and Table S1). Bubble-like lesions could occur along the length of the touch neuron processes (Fig. 1*E*). Beading represented focal enlargement along the nerve process (Fig. 1*F*). Blebs, triangular-shape protrusions from the touch neuron processes, often led to distortion of the gross structure (Fig. 1*H*). In extremely old animals [days of adulthood 20 (D20) or older], slender branches developed from the blebs (Fig. 1*I*). Beading and bubble-like lesions occurred in both the ALM and the PLM, whereas blebs and branching occurred most frequently in the PLM. These age-dependent defects were also seen in the AVM and PVM touch neurons. We confirmed these observations with a second GFP reporter and also by acetylated α-tubulin staining (Fig. S1 *A* and *B*). Axon beading or blebs were not labeled by antibodies against Rab7, a marker for late endosome and lysosome (Fig. S1 *E–J*). We occasionally observed splitting of the touch neuron processes that coexisted with blebs or bubble-like lesions (Fig. S1 *C* and *D*). This leads us to speculate that some of the blebs or bubble-like lesions may represent an early phase of axon splitting. The frequency of these abnormalities increases with age (Fig. 1 *C*, *J*, and *K*). Importantly, even in touch neurons with marked somatic and axonal defects, the nuclear DAPI staining was intact and never appeared fragmented (Fig. S1 *K* and *L*), suggesting that these aged neurons were not in the process of apoptosis or necrosis.

Author contributions: C.-L.P. and S.M. designed research; C.-L.P., C.-Y.P., and C.-H.C. performed research; C.-L.P., C.-Y.P., C.-H.C., and S.M. analyzed data; and C.-L.P. and S.M. wrote the paper.

The authors declare no conflict of interest.

This article is a PNAS Direct Submission.

[1]To whom correspondence may be addressed. E-mail: chunliangpan@gmail.com and slm@gallo.ucsf.edu.

This article contains supporting information online at www.pnas.org/lookup/suppl/doi:10.1073/pnas.1011711108/-/DCSupplemental.

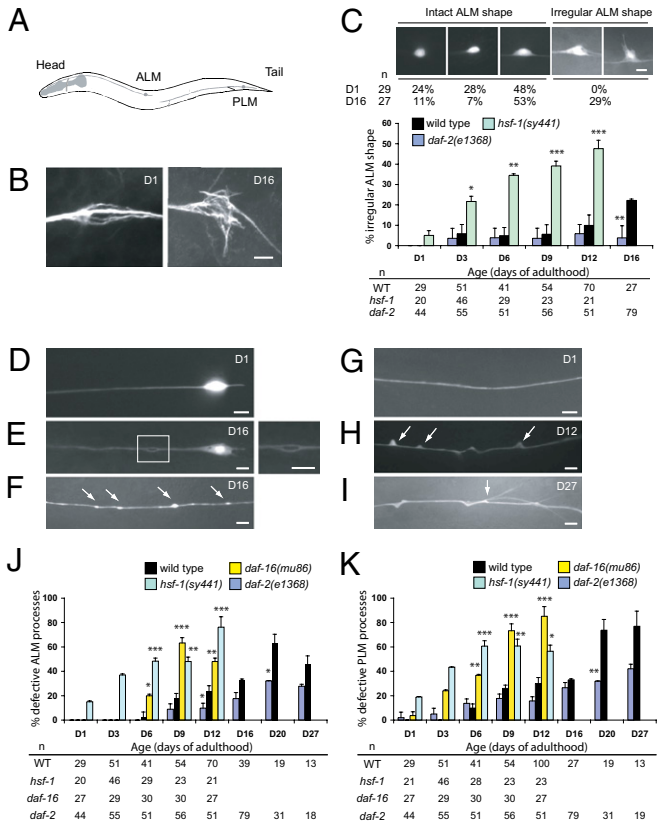

Fig. 1. Age-dependent defects occur in *C. elegans* touch receptor neurons. (Scale bar: 5 μm.) (*A*) Diagram of *C. elegans* paired ALM and PLM touch receptor neurons (lateral view). Only neurons on the left are shown. (*B*) Immunostaining of the wild-type ALM neuronal cell bodies with the anti-acetylated α-tubulin antibody 6–11B-1. The age of the animals (days of adulthood) is indicated. (*C*) Quantification of ALM neurons with irregularly shaped soma in the wild type and the mutants. Representative GFP images of different wild-type ALM neuronal shapes are shown, with number of neurons scored (*n*) at each time point. GFP is from *zdIs5(Pmec-4::gfp)*. (*D–I*) Epifluorescence images of age-dependent defects of the ALM (*D* and *E*) and the PLM (*F–I*) processes in wild type. Anterior is to the left. (*E*) A bubble-like lesion in the ALM process. *Inset* is enlarged on the right. Beading (*F*, arrows), blebbing (*H*, arrows), and branching (*I*) of the PLM process are shown. Branching appears to develop from the sites of blebbing (*I*, arrow). (*J* and *K*) Quantification of the ALM (*J*) and the PLM (*K*) process abnormalities in wild-type and mutant adult animals. Error bars are SEs of proportions. The number of neurons scored (*n*) at each time point is provided. $*P < 0.05$, $**P < 0.01$, and $***P < 0.001$ (Fisher's exact test or two-proportion test).

To test whether age-related defects are specific to touch neurons, we examined cholinergic axons in the ventral nerve cord (VNC), a pair of longitudinal nerve tracts that extend from the head to the tail. VNC cholinergic axons of young adult animals travel along the antero-posterior axis in two discrete fascicles on the right side, and individual axons are tightly packed into either fascicle (Fig. S2*A*). In middle age (D6–D8), however, occasionally three, instead of two, cholinergic nerve fascicles were observed in the right VNC (Fig. S2*B*). The length of the supernumerary processes and the invariant anterior–posterior orientation suggest that these were defasciculated axons rather than aberrant neuronal sprouts. VNC defasciculation became more pronounced, and axon beading developed in animals of advanced age (D14–D17) (Fig. S2 *B* and *E*). These results indicate that age-dependent morphological defects occur in multiple classes of *C. elegans* neurons.

Longitudinal Imaging of *C. elegans* Touch Neurons During Aging. To understand how age-dependent defects evolve in touch neurons over time, we performed longitudinal imaging on individual ALM neurons over the animal's life span (Fig. 2). The onset of growth of aberrant protrusions is variable, and they may persist or retract from the cell body briefly after their appearance (Fig. 2*A*). The posterior process of ALM sometimes branched in middle age (Fig. 2*B*). We also documented the formation of bubble-like lesions (Fig. 2*A*). A segment of the ALM process first became distended, and several foci devoid of axoplasmic GFP fluorescence subsequently coalesced to form a single large bubble-like structure, which could continue to expand (Fig. 2*A*). We observed disappearance of the bubble-like lesion 1 d before the animal died, accompanied by a thinning and disassembly of the ALM process (Fig. 2*A*). These observations highlight the transient and dynamic nature of morphological defects in aging touch neurons. In contrast to axon regeneration after laser axotomy (reviewed in ref. 11), the age-dependent morphological decline of *C. elegans* neurons seen in our longitudinal studies was slow, and we did not observe neuronal behaviors indicative of regeneration.

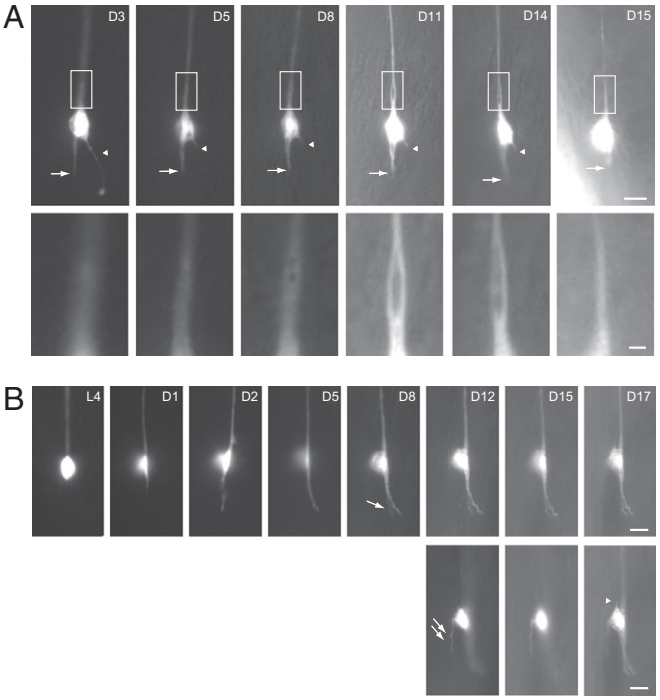

Fig. 2. Longitudinal imaging of ALM neurons in the wild type. Epifluorescence images of individual ALM neurons at different time points over the animals' life span (lateral view); anterior is up and ventral side is to the right. GFP is from *zdIs5(Pmec-4::gfp)*. Ages (days of adulthood) are indicated. [Scale bar: 5 μm or 1 μm (*A*, *Insets*).] (*A*) The posterior process of the ALM neuron (arrow), which became slightly shorter and thicker between D3 and D5, remained static from D5 to D14, and retracted on D15. Arrowheads indicate an aberrant protrusion from the cell body, which was truncated between D3 and D5, and completely disappeared on D15. *Insets* highlight the development of a bubble-like structure at the proximal segment of the ALM process. The animal died on D16. (*B*) The posterior process of the animal grew out on D1, continued to extend between D1 and D5, and branched at D8 (single arrow). An aberrant protrusion developed from the dorsal side of the cell body at D12 (double arrows). On D17, another short protrusion developed at the anterior pole of the ALM neuron (arrowhead). (*Lower*) The three images were taken from different focal planes compared with their temporal counterparts in the *Upper*.

NEUROSCIENCE

Age-Dependent Neuronal Defects Are Modified by Genes That Control the Life Span. Genes that control *C. elegans* life span also control age-dependent tissue degeneration. Tissue degeneration is delayed in the long-lived *daf-2* mutant and is accelerated in the short-lived *daf-16* mutant (2, 4). The FOXO transcription factor DAF-16 mediates the longevity effects of mutations in *daf-2*, which encodes the sole insulin-like growth factor receptor homolog in *C. elegans* (12). We hypothesize that age-dependent neuronal defects are also regulated by mutations that affect life span.

We first examined the long-lived *daf-2* mutants and found that age-dependent defects of touch neurons and VNC cholinergic axons were significantly delayed (Fig. 1 *C*, *J*, and *K* and Fig. S2). By contrast, the frequency of touch neuron defects was significantly increased in the short-lived *daf-16(mu86)* mutants (Fig. 1 *J* and *K*). The development of touch neurons in *daf-16* mutants was normal, indicating that *daf-16* neuronal phenotypes represent premature aging rather than developmental abnormalities. These results indicate that insulin signaling regulates morphological aging of touch neurons in *C. elegans*.

We next examined mutations that affect aging independently of insulin signaling. Mutations in the *eat-2* nicotinic cholinergic receptor reduce pharyngeal pumping rate and promote moderate life-span extension (13), and the *eat-2(ad465)* mutant did not display premature neuronal aging. Mutations in *hsf-1*, which encodes the heat-shock transcription factor that mediates cellular responses to heat stress, shorten life span (14). We found that the loss-of-function *hsf-1(sy441)* mutation accelerated neuronal aging (Fig. 1 *C*, *J*, and *K* and Fig. S2 *C–E*). Age-dependent defects of touch neurons were not enhanced in the *daf-16 hsf-1* double mutants, suggesting that these two genes largely act in the same pathway for neuronal aging (Fig. S3*A*). Similarly, mutations in the nuclear lamin gene *lmn-1* shortened life span and triggered neuronal aging (*SI Results*).

The morphological features of neuronal defects in the short-lived *daf-16* and *hsf-1* mutants were indistinguishable from those in aged wild-type worms, indicating that the observed neuronal defects in the *daf-16* and *hsf-1* mutants represented accelerated aging, which is supported by our longitudinal imaging (Fig. S4). Restoration of DAF-16 functions specifically in the neurons or in the body-wall muscles did not rescue the age-dependent touch neuron defects of the *daf-16(mu86)* mutant, indicating that DAF-16 acts outside the nervous system to regulate neuronal aging in *C. elegans* (Fig. S3*B*).

Touch Neuron Defects in Mutants Defective for Touch Sensitivity. To test whether evoked activity is required for the maintenance of touch neurons, we examined mutants in which touch-evoked sensory transduction in these neurons was absent (also known as

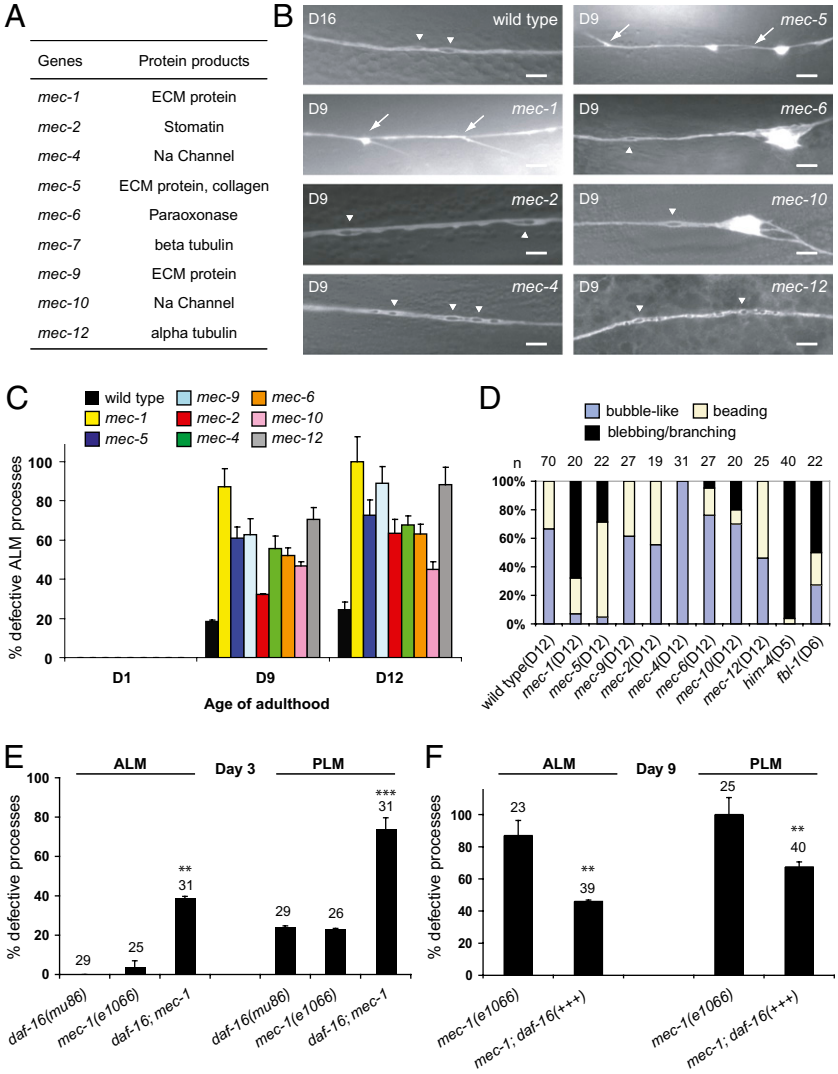

Fig. 3. Progressive touch neuron defects in the *mec* mutants. (*A*) Summary of the *mec* genes and their encoded proteins. (*B*) Representative live GFP images (except for that of the *mec-12* mutant, which is immunofluorescence image-labeled by 6–11B-1) of the ALM processes in the wild type (D16) and the mutants (D9). (Scale bar: 5 μm.) Arrows and arrowheads indicate branching and bubble-like lesions, respectively. (*C*) Quantification of defective ALM processes. Total numbers of ALM neurons scored (D1/D9/D12): wild type, 29/54/70; *mec-1*, 25/23/20; *mec-2*, 17/28/19; *mec-4*, 24/18/31; *mec-5*, 31/23/22; *mec-6*, 19/25/27; *mec-9*, 20/16/27; *mec-10*, 23/29/20; *mec-12*, 19/27/25. (*D*) Percentages of bubble-like lesions, beading, or blebbing/branching in all of the abnormal events found in the ALM neurons of wild type and the mutants. The age of the animals is specified. (*E*) Defects of the ALM and the PLM processes of D3 *mec-1(e1066)* mutants are enhanced by a *daf-16 (mu86)* mutation. (*F*) Overexpression of DAF-16 from the endogenous *daf-16* promoter significantly suppresses ALM and PLM defects of D9 *mec-1(e1066)* mutants. Error bars are SEs of proportions. $^{**}P < 0.01$ or $^{***}P < 0.001$ (Fisher's exact test or two-proportion test).

the Mec phenotype) (10, 15) (Fig. 3*A*), while responses to harsh mechanical stimulation are retained. We found that touch neurons in the *mec* mutants developed normally, but displayed significant defects starting from mid-adulthood and increasing with age (Fig. 3 *B* and *C*). Although mutations in *mec-2*, *mec-4*, *mec-5*, *mec-6*, *mec-9*, and *mec-10* caused a shortened life span, those in *mec-1* and *mec-12* did not (Fig. S5). This indicates that *mec-1* and *mec-12* mutations specifically induce age-dependent neuronal defects without affecting the general aging process. In support of this hypothesis, we found that a *daf-16* mutation significantly increased touch neuron defects in *mec-1* animals (Fig. 3*E*). Overexpression of DAF-16, by contrast, significantly rescued the neuronal aging phenotypes of *mec-1* mutants (Fig. 3*F*). These results indicate that activities of DAF-16 and MEC-1 act synergistically to maintain the integrity of touch neurons.

Age-dependent neuropathology of the *mec* mutants could be further divided into two types. Type 1 pathology was characterized by beading and bubble-like lesions of the ALM processes, which were similar to the aging phenotypes in wild-type animals (Fig. 3 *B* and *D*). Mutations in genes that encode the touch mechanosensory channel components MEC-2, MEC-4, MEC-6, and MEC-10 (10, 16–18), the extracellular matrix (ECM) protein MEC-9 (19), and the α-tubulin MEC-12 (10) led to type 1 pathology (Fig. 3 *A*, *B*, and *D*). By contrast, type 2 pathology was characterized by blebbing, branching, and distortion of the nerve processes. Mutations in genes that encode the unique ECM proteins MEC-1 and MEC-5 (19, 20) led to type 2 pathology (Fig. 3 *A*, *B*, and *D*). These abnormal branches contained acetylated microtubules (Fig. S6 *A* and *B*).

Disruption of Nerve Attachment Leads to Blebbing and Branching of the Touch Neuron Processes. To our surprise, not all *mec-1* mutations led to type 2 pathology. *mec-1(e1066)* and *mec-1(e1292)*, which are predicted to truncate significant portions of the N-terminal region containing multiple EGF and Kunitz domains (20), caused type 2 pathology (Fig. 4 *B* and *G* and Fig S6*B*). By contrast, *mec-1(e1526)*, which eliminates the C-terminal domain and the last Kunitz domain (20), caused type 1 pathology (Fig. 4 *B* and *H* and Fig. S7*B*).

The aforementioned differences in neuronal defects could not be explained by a disruption in sensory-evoked activity, as these mutants were similarly impaired for touch sensitivity. In wild type, the processes of touch receptor neurons are engulfed by the neighboring epithelial cells and are separated from the body-wall muscles (20). Subsequently, hemidesmosome-like structures form in the squamified epithelial cell cytoplasm that overlies the touch neuron process, which completes the process of nerve attachment. In the *mec-1(e1066)* mutant, touch neuron processes failed to separate from body-wall muscles, and normal nerve attachment did not form (10, 20) (Fig. 4 *A*–*D*). We found that nerve attachment was also disrupted in the *mec-1(e1292)* mutant. By contrast, the *mec-1(e1526)* mutant had intact nerve attachment (Fig. 4*E*). These results suggest that disruption of nerve attachment leads to type 2 pathology in the touch receptor neurons.

To test this hypothesis, we examined nerve attachment in representative mutants leading to type 1 or type 2 pathology. We found that, in the *mec-4* and the *mec-9* mutants, which showed type 1 pathology, nerve attachment was intact (Fig. S7 *D* and *E*). By contrast, in the *mec-5* mutant, which displayed type 2 pathology, nerve attachment was disrupted (Fig. S7*C*). Some *mec-5* mutants retained partial nerve attachment, consistent with the fact that branching phenotypes of the *mec-5* mutant were less severe than those of the *mec-1(e1066)* mutant (Fig. 3*C*).

We further tested two mutants with normal touch sensitivity but defective nerve attachment, *him-4* and *fbl-1*, which encode the ECM proteins hemicentin and fibulin, respectively (21, 22). The *him-4(rh319)* null mutants phenocopied the *mec-1(e1066)* and the *mec-1(e1292)* mutants, displaying characteristic blebbing and branching defects of ALM and PLM (Fig. S6 *C*–*F* and *I*). Because the *fbl-1(hd43)* homozygotes were almost completely sterile, we examined *fbl-1* homozygotes that segregated from the *fbl-1* heterozygotes and thus retained the maternal FBL-1 components (*fbl-1* M+Z−). In the *fbl-1(hd43)*(M+Z−) mutants, early onset of adult touch receptor neuron defects was found, with comparable frequency of type 1 and type 2 pathology (Fig. 3*D* and Fig. S6 *G*, *H*, and *J*). Taken together, these results indicate that disruption of nerve attachment induces blebbing and branching in the adult touch neurons.

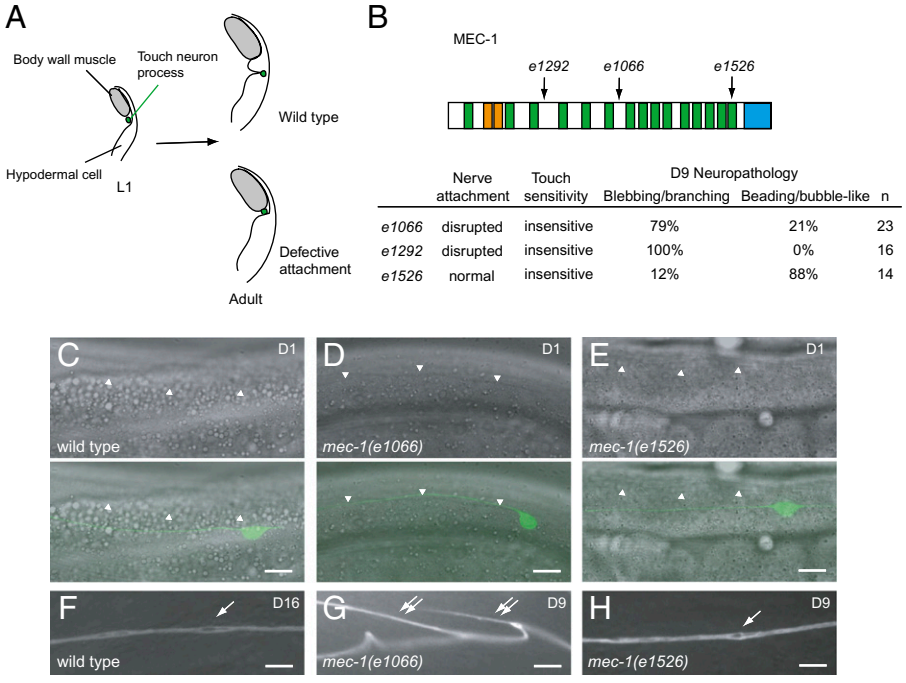

	Nerve attachment	Touch sensitivity	D9 Neuropathology Blebbing/branching	Beading/bubble-like	n
e1066	disrupted	insensitive	79%	21%	23
e1292	disrupted	insensitive	100%	0%	16
e1526	normal	insensitive	12%	88%	14

Fig. 4. Disruption of nerve attachment or neuronal activity causes distinctive degeneration phenotypes. (Scale bar: 10 μm.) (*A*) Diagram of touch neuron attachment (transverse section). In wild-type L1 larvae, the process of the touch receptor neuron lies adjacent to the body-wall muscles. The nerve process later adopts the adult position where it is attached to the overlying cuticle and is thus separated from the muscles. In mutants with defective attachment, the touch neuron process remains in the juvenile position and is not attached to the epithelium. (*B*) MEC-1 protein structure. *e1066*, splice junction mutation; *e1292*, nonsense mutation; *e1526*, missense mutation. Orange, EGF domains; green, Kunitz domains; blue, the C terminus domain. Percentages of the predominant type defects (branching/blebbing or bubble-like/beading) of all axonal defects are provided. (*C*–*E*) Attachment of the ALM process in wild-type (C) and *mec-1* mutants (*D* and *E*). (*Upper* panels) Differential interference contrast (DIC) images. (*Lower* panels) Overlay of DIC and GFP images. The lower borders of body-wall muscles are indicated by arrowheads. (*F*–*H*) Representative pathology of aging ALM neurons in wild-type (*F*) and *mec-1* mutants (*G* and *H*). Single arrows: bubble-like lesions. Double arrows: branching of the nerve processes.

Evoked Activity Is Required for the Maintenance of Adult Touch Neurons. Our mutant analysis suggests that sensory-evoked activity is required for the maintenance of adult touch neurons. To test this hypothesis further, we inactivated touch neurons by using a hyperpolarizing ion channel. The outward hyperpolarizing BK potassium channel SLO-1 is broadly expressed in the *C. elegans* neurons (23). In the *slo-1* gain-of-function mutants *slo-1(ky389)* and *slo-1(ky399)* (24, 25), touch sensitivity was partially defective, suggesting that touch-evoked sensory transduction was impaired. Early onset, progressive touch neuron defects were found in both *slo-1(ky389)* and *slo-1(ky399)* mutants, including the formation of bubble-like lesions and axon beading (Fig. 5). Touch neuron somas in these mutants began to degenerate in early adulthood, characterized by a disorganization in shape, breakdown of microtubule bundles, and eventually complete disappearance of cell bodies (Fig. 5). Overexpression of wild-type SLO-1 in the neurons using the *snb-1*/synaptobrevin promoter also induced similar phenotypes (Fig. 5). To show that the requirement for evoked activity in neuronal maintenance is not a unique property of the touch neurons, we examined the effects of altered synaptic transmission on adult GABAergic DD and VD motor neurons. Blockade of synaptic transmission presumably eliminates evoked activities in these neurons, whereas augmented synaptic transmission facilitates neuronal activation. In wild type, DD and VD neurons display age-dependent axon beading in both the ventral and the dorsal nerve cord (Fig. S8). Mutations in *unc-13* and *unc-18*, which are required for active zone functions and membrane targeting of UNC-64/syntaxin, respectively, disrupt synaptic transmission. In the *unc-13* and *unc-18* mutants, DD and the VD axons in the ventral and dorsal nerve cords developed progressive beading as the animals aged (Fig. S8). Mutations in *dgk-1*, which encodes a diacylglycerol kinase that dampens synaptic transmission through phosphorylation of diacylglycerol, enhanced synaptic activities. Compared with the wild type, GABAergic axons in the ventral and dorsal nerve cords of *dgk-1* mutants were relatively preserved at advanced age (Fig. S8). Taken together, these results support the hypothesis that evoked activity is required for the maintenance of adult postmitotic neurons in *C. elegans*.

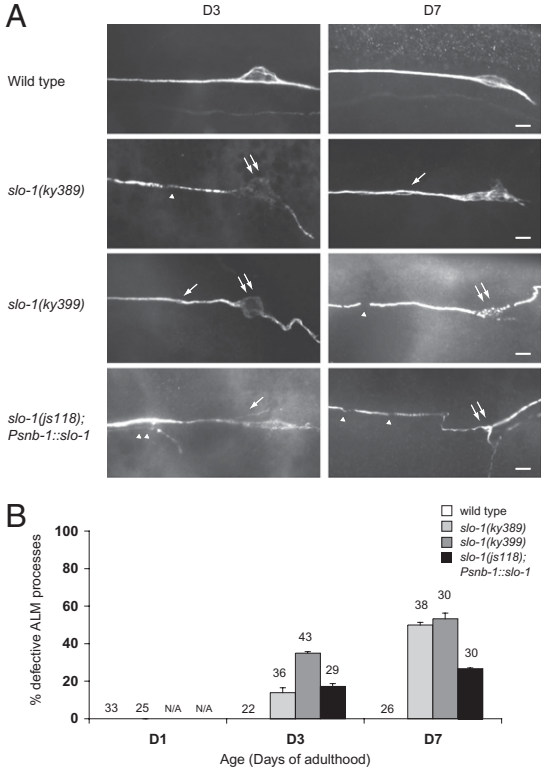

Fig. 5. Suppression of electrical activity by *slo-1* gain-of-function mutations induces progressive touch receptor neuron defects. (Scale bar: 5 μm.) (*A*) Immunofluorescence images of ALM neurons in the wild-type, *slo-1(ky389)*, *slo-1(ky399)*, and *slo-1(js118); Psnb-1::slo-1* animals at D3 and D7 of adulthood, with touch receptor neurons labeled by the 6–11B-1 antibody. *ky389* and *ky399* are gain-of-function mutations, and *js118* is a recessive loss-of-function mutation. Acetylated tubulin was decreased and disorganized in the neuronal cell bodies in *slo-1(ky389)*, *slo-1(ky399)*, and *slo-1(js118); Psnb-1::slo-1* mutants. Single arrows: bubble-like lesions; single arrowheads: discontinuity of the acetylated tubulin immunoreactivity; double arrows: ALM cell bodies; double arrowheads: branching from the nerve processes. (*B*) Quantification of ALM defects in wild type, *slo-1(ky389)*, *slo-1(ky399)*, and *slo-1(js118); Psnb-1::slo-1* animals at D1, D3, and D7. Error bars are SEs of proportions. The number of cells scored is indicated. N/A, not available.

Discussion

A recent report shows that, although the numbers of neurons are preserved, loss of neuronal and dendritic architectures are likely responsible for the cortical thinning and brain atrophy in the normally aging human brain (26). Together with the findings presented in the current study, we conclude that alterations in neuronal cytoarchitecture are hallmarks of aging in both the vertebrate and the invertebrate nervous systems.

Our observation that nerve attachment is essential for the maintenance of adult touch receptor neurons reveals a previously unidentified role for this developmental process. Nerve attachment is neither necessary nor sufficient for touch sensitivity, as attachment-defective *him-4* and *fbl-1* mutants show nearly normal touch response, and the attachment-intact *mec-1(e1526)* mutant is touch-insensitive (20–22). Our results are consistent with a model where HIM-4, MEC-1, and MEC-5 function in a common pathway for touch neuron attachment, which in turn is required for the maintenance of adult touch neuron integrity. Attachment of the nerve processes may protect them from mechanical strains during movements. Alternatively, ECM proteins may function to stabilize the neuronal membrane and the cytoskeleton via their interactions with membrane receptors and cytoskeleton adaptors in the neurons. Although no MEC-1 homologs have been identified in species other than *C. elegans* and *Caenorhabditis briggsae*, mutations in human hemicentin, the *C. elegans* homolog of which is HIM-4, have been associated with age-dependent macular degeneration, consistent with their functions in the maintenance of adult tissue integrity (27).

We demonstrated that disrupted evoked activity or reduced neuronal excitability accelerates aging of the touch neurons. Disrupting the mechanosensory channel components abolished the evoked touch current in the neurons, and a mutation in the α-tubulin MEC-12, *e1605*, also significantly reduced this current (15, 28). Overactivation of the hyperpolarizing potassium channel SLO-1 impaired neuronal excitability and triggered progressive neuronal defects. Because *slo-1* is broadly expressed in the nervous system, the effects of excessive SLO-1 activity on the maintenance of touch neurons could be cell-autonomous, or it could act in other neurons and impact touch neurons indirectly. We also noted that, in animals with excessive SLO-1 activity, acetylated microtubule immunoreactivity sometimes became discontinuous in the process or was significantly diminished in the soma of touch neurons. These findings were rare in aging wild-type touch neurons, suggesting that SLO-1 activity may impair neuronal structure via a hyperpolarization-independent mechanism. Nonetheless, together with the observation that altered synaptic transmission affects adult neuronal integrity, these data support the hypothesis that a reduction in neuronal activity likely contributes to morphological alterations during neuronal aging. *unc-13* and *unc-18* mutations did not trigger premature aging in the touch neurons, probably because they are not postsynaptic to other neurons, and their evoked activity is in-

dependent of synaptic release. Interestingly, a dominant, gain-of-function *mec-4* mutation [*mec-4(d)*], which constitutively activates the MEC-4 Na^+ channel, causes the touch neurons to develop enormous cytoplasmic vacuoles and die rapidly (18), probably caused by massive ion influx and subsequent activation of proteolytic enzymes (29). These results indicate that the overall level of activity is critical for the survival or maintenance of neurons. Identification of the transcriptional targets of electrical activity in the maintenance of adult neurons during aging may facilitate the development of therapeutics that effectively modify the progression of age-dependent neurodegenerative diseases.

Materials and Methods

C. elegans strains were cultured under established conditions. Information on alleles and integrated arrays, FUDR treatment, and immunofluorescence microscopy are in *SI Materials and Methods*.

Longitudinal Fluorescence Microscopy. Individual animals were immobilized with levamisole and imaged under a Zeiss Axioskop microscope. Animals were rescued from the slides after imaging, placed on plates with bacterial food, washed with several drops of physiological M9 buffer, and allowed to recover. The imaging procedure took less than 2 min and was well tolerated by the animals. The same sides were repeatedly imaged for individual animals at defined time points along the animal's life span. A total of 17 wild-type animals were recorded, and the maximal ages of recorded animals are the following: D17, $n = 3$; D16, $n = 1$; D15, $n = 4$; D14, $n = 4$; D12, $n = 1$, and D9, $n = 3$. One animal died after two imaging sessions on D1 from an unknown cause. In sum, 13 of 17 (76%) of the animals could be repeatedly imaged until D12 or older.

ACKNOWLEDGMENTS. We thank Cori Bargmann, Gian Garriga, Miriam Goodman, Barth Grant, Joshua Kaplan, Cynthia Kenyon, Bruce Vogel, June-Tai Wu, and the *Caenorhabditis* Genetics Center for providing some of the strains and reagents used in this study and Andre Ho and Yi-Chun Wu for assistance with microinjection. We thank Gian Garriga, Jason Chien, Matthew Schreiber, and Fred Wolf for critical reading and comments on the manuscript. This work was supported by National Science Council (Taiwan) Grant NSC 99-2320-B-002-080 (to C.-L.P.) and funding from the state of California for medical research on alcohol and substance abuse through the University of California at San Francisco (to S.M.).

1. Yankner BA, Lu T, Loerch P (2008) The aging brain. *Annu Rev Pathol* 3:41–66.
2. Garigan D, et al. (2002) Genetic analysis of tissue aging in Caenorhabditis elegans: A role for heat-shock factor and bacterial proliferation. *Genetics* 161:1101–1112.
3. Herndon LA, et al. (2002) Stochastic and genetic factors influence tissue-specific decline in ageing C. elegans. *Nature* 419:808–814.
4. Haithcock E, et al. (2005) Age-related changes of nuclear architecture in Caenorhabditis elegans. *Proc Natl Acad Sci USA* 102:16690–16695.
5. Collins JJ, Huang C, Hughes S, Kornfeld K (2008) The measurement and analysis of age-related changes in Caenorhabditis elegans. *WormBook*, Jan 24:1–21.
6. Cai SQ, Sesti F (2009) Oxidation of a potassium channel causes progressive sensory function loss during aging. *Nat Neurosci* 12:611–617.
7. Spitzer NC (2006) Electrical activity in early neuronal development. *Nature* 444: 707–712.
8. Lin CW, et al. (2010) Genetically increased cell-intrinsic excitability enhances neuronal integration into adult brain circuits. *Neuron* 65:32–39.
9. Chiang A, Priya R, Ramaswami M, Vijayraghavan K, Rodrigues V (2009) Neuronal activity and Wnt signaling act through Gsk3-beta to regulate axonal integrity in mature Drosophila olfactory sensory neurons. *Development* 136:1273–1282.
10. Chalfie M, Sulston J (1981) Developmental genetics of the mechanosensory neurons of Caenorhabditis elegans. *Dev Biol* 82:358–370.
11. Wang Z, Jin Y (2011) Genetic dissection of axon regeneration. *Curr Opin Neurobiol* 21: 189–196.
12. Kenyon CJ (2010) The genetics of ageing. *Nature* 464:504–512.
13. Avery L (1993) The genetics of feeding in Caenorhabditis elegans. *Genetics* 133: 897–917.
14. Hsu AL, Murphy CT, Kenyon C (2003) Regulation of aging and age-related disease by DAF-16 and heat-shock factor. *Science* 300:1142–1145.
15. Chalfie M (2009) Neurosensory mechanotransduction. *Nat Rev Mol Cell Biol* 10:44–52.
16. Chalfie M, Au M (1989) Genetic control of differentiation of the Caenorhabditis elegans touch receptor neurons. *Science* 243:1027–1033.
17. Chelur DS, et al. (2002) The mechanosensory protein MEC-6 is a subunit of the C. elegans touch-cell degenerin channel. *Nature* 420:669–673.
18. Driscoll M, Chalfie M (1991) The mec-4 gene is a member of a family of Caenorhabditis elegans genes that can mutate to induce neuronal degeneration. *Nature* 349:588–593.
19. Du H, Gu G, William CM, Chalfie M (1996) Extracellular proteins needed for C. elegans mechanosensation. *Neuron* 16:183–194.
20. Emtage L, Gu G, Hartwieg E, Chalfie M (2004) Extracellular proteins organize the mechanosensory channel complex in C. elegans touch receptor neurons. *Neuron* 44: 795–807.
21. Vogel BE, Hedgecock EM (2001) Hemicentin, a conserved extracellular member of the immunoglobulin superfamily, organizes epithelial and other cell attachments into oriented line-shaped junctions. *Development* 128:883–894.
22. Muriel JM, Dong C, Hutter H, Vogel BE (2005) Fibulin-1C and fibulin-1D splice variants have distinct functions and assemble in a hemicentin-dependent manner. *Development* 132:4223–4234.
23. Wang ZW, Saifee O, Nonet ML, Salkoff L (2001) SLO-1 potassium channels control quantal content of neurotransmitter release at the C. elegans neuromuscular junction. *Neuron* 32:867–881.
24. Troemel ER, Sagasti A, Bargmann CI (1999) Lateral signaling mediated by axon contact and calcium entry regulates asymmetric odorant receptor expression in C. elegans. *Cell* 99:387–398.
25. Davies AG, et al. (2003) A central role of the BK potassium channel in behavioral responses to ethanol in C. elegans. *Cell* 115:655–666.
26. Freeman SH, et al. (2008) Preservation of neuronal number despite age-related cortical brain atrophy in elderly subjects without Alzheimer disease. *J Neuropathol Exp Neurol* 67:1205–1212.
27. Schultz DW, et al. (2003) Analysis of the ARMD1 locus: Evidence that a mutation in HEMICENTIN-1 is associated with age-related macular degeneration in a large family. *Hum Mol Genet* 12:3315–3323.
28. Bounoutas A, O'Hagan R, Chalfie M (2009) The multipurpose 15-protofilament microtubules in C. elegans have specific roles in mechanosensation. *Curr Biol* 19: 1362–1367.
29. Kourtis N, Tavernarakis N (2007) Non-developmentally programmed cell death in Caenorhabditis elegans. *Semin Cancer Biol* 17:122–133.